OTC 6970

Drag Embedment Anchor Performance Prediction in Soft Soils

W.P. Stewart, Stewart Technology Assocs.

This paper was presented at the 24th Annual OTC in Houston, Texas, May 4–7, 1992.

ABSTRACT

A rational approach to calculating the drag embedment performance of marine anchors in cohesive soils is presented. The method considers the geotechnical and gravity/buoyancy forces acting on all components of the anchor system including various areas on the anchor and the attached mooring line which may be either chain or wire. The solution proceeds in a piece-wise linear manner until an equilibrium position is found for the anchor. This equilibrium position is described in terms of the anchor burial depth, the anchor drag distance, and an anchor angle of rotation in the soil. The equilibrium position may be such that the anchor holds the applied line load and no further movement occurs, or it may be such that the anchor can dig no deeper and horizontal movement is predicted with a given maximum resistance.

The solution technique requires a computer program. Such program has been developed and the results from the program have been compared with large scale tests performed in the Gulf of Mexico in 1990.

HISTORICAL ANCHOR DESIGN

This paper is concerned primarily with relatively large marine drag embedment type anchors which are used in the offshore industry. However, it is worth considering the evolution of anchors in general. The first patent that was filed for describing an anchor was that by Hawkins in 1821. This patent described an anchor consisting of two flukes which were articulated about a pin perpendicular to the shank of the anchor. This concept has remained in use today and falls now into two main categories of stockless anchors and stock anchors.

Stockless anchors are widely used today on warships and on merchant ships. They are not typically used in the offshore industry.

Articulated stock anchors are more widely used in commercial applications today than stockless anchors. The Danforth anchor is a typical example developed in the late 1930s. These anchors are used on barges and semi-submersible drilling rigs. Names in common use include Danforth, LWT, and Offdrill.

The requirements of the offshore industry to provide ever larger capacities of anchors led to a scaling up of existing models. Stockless and stock anchors weighing up to 30 tons in air have been built. Special anchor handling vessels have been developed specifically for the placement and retrieval of these anchors. In the last decade, the increasing use of permanent mooring systems for floating production has resulted in the design of anchors specialized to certain types of soil conditions. In the soft cohesive soils typical of many deep water areas in the world, increasing use of anchors fabricated from steel plates has occurred. These fabricated anchors replace cast steel anchors. They are more efficient in terms of their holding capacity compared to their weight. However, they are very specific to individual applications and cannot be regarded as general purpose anchors.

References and figures at end of paper

TRADITIONAL ASSESSMENT OF ANCHOR CAPACITIES

In the offshore industry, the capacity of anchors has traditionally been assessed (in the last decade or so) by reference to curves relating anchor weight to anchor holding capacity. Such curves are included in API Recommended Practices and largely emanate from tests performed by the Naval Civil Engineering Laboratory (NCEL). There has been a widespread belief in industry that the maximum capacity of an anchor system (which comprises a mooring line and an anchor) can be achieved if heavy chain is used rather than wire rope. The NCEL curves have normally been produced with tests where chain has been attached to the anchor being tested. The advantages of using chain rather than wire for the section of mooring line attached to the anchor include the increased ability of chain to resist wear caused by dynamic contact with the sea bed soil and the extra weight of the chain (compared to the same strength wire) which results in reduced uplift forces from the mooring catenary to the sea bed section of the mooring line. Additionally, chain has an increased frictional resistance with the sea bed soil when compared to wire both because of its geometrical shape and because of its larger weight. However, there is now an increased awareness that anchor capacities are limited, especially in soft cohesive soils (where undrained shear strength tends to increase with depth) by the depth of embedment that any anchor can achieve. The principal resistance to embedment for a well designed anchor comes from the vertical component of force which the anchor line applies to the anchor shackle at the shank of the anchor. As an anchor buries deeper, more and more line must be pulled down into the sea bed with the anchor. Eventually, there comes a point where further embedment of the anchor vertically can no longer occur as the anchor line applies a vertical force which is greater than the geotechnical and weight forces demanding embedment.

STAGES IN ANCHOR EMBEDMENT

Depending upon the anchor type being analyzed, up to four stages of anchor embedment, sometimes referred to as anchor kinematics, can be defined. These phases are successive and as shown below:

1. *Opening of the flukes (if the anchor is an articulated type).*
2. *Penetration of the flukes.*
3. *Burial of the anchor, including the flukes, shank, and anchor line.*
4. *Stable or unstable embedment during dragging, becoming depth limited by geotechnical forces on the anchor line.*

Much of the art of the design of anchors has been associated with the evolution of successful tripping "mechanisms" and/or fluke geometry to encourage tripping. The tripping angle is usually defined as the angle at which the flukes enter the soil and penetration begins. Anchor designers have employed various means to ensure that penetration will occur in different soil types. Some anchors have unstable penetration in certain soils, which may be exhibited as "rolling while dragging", resulting in a lack of satisfactory embedment. For further information on the kinematics of anchors and their initial penetration behavior, the reader is referred to Puech, Reference 1.

This paper is concerned with the burial phase of anchor performance and the prediction of maximum anchor capacity in cohesive soils. A two-dimensional analysis is used. Instabilities such as "rolling while dragging" cannot be analyzed by this method.

FORCES ON ANCHOR LINES

Figure 1 shows the forces imposed upon a buried section of anchor line in a cohesive soil. From this figure, it is seen that there is a tangential component of force caused by the soil adhesion to the line and a normal component of force from the soil bearing pressure on the line. These forces, together with the applied line tension and the anchor resistance, result in a curved geometry for the line in the side view as shown in Figure 1. In order to calculate the line geometry and the changes in tension along the length of the line, a procedure has been developed to divide the line into elemental lengths. At each elemental location, the line tension forces and line weight are balanced by soil forces (References 2, 3 and 4). Referring to Figure 2, we have the following relationships.

$$dT/ds = - t - w.\sin(\theta) \quad (1)$$

$$d\theta/ds = [q - w.\cos(\theta)]/T \quad (2)$$

$$q = N_c.c_u.A_b \quad (3)$$

$$t = c_u.A_s \quad (4)$$

Where:

dT	=	tension change over element length
T	=	mean line tension at element
ds	=	element length
t	=	tangential soil force per unit length
w	=	line unit weight per unit length
$d\theta$	=	line angle change over element length
q	=	normal soil force on line per unit length
N_c	=	bearing capacity coefficient
c_u	=	undrained shear strength of the soil
A_b	=	line area bearing on soil per unit length
A_s	=	line surface area per unit length

From the above relationships, it is possible to calculate the tensions and positions at each element in a "finite element model" of the mooring line in the cohesive soil. It should be noted that the mathematical model built in this way can account for the mooring line leaving the sea bed at any angle, varying from the horizontal to being completely vertical.

SOIL MODELLING

The embedment depth of modern fabricated steel plate anchors can be surprisingly large if they are embedded using a wire forerunner rather than chain. Embedment depths in the range of six to eight times the fluke length have been achieved in large scale pull tests involving two ton and seven ton anchors in the Gulf of Mexico. Such tests were conducted by Omega Marine International, Inc., in the summer of 1990. The geotechnical properties of cohesive soil which are important for the calculation of drag anchor performance are principally the undrained shear strength, c_u, and the buoyant weight of the soil, γ_b. Additionally, it is important to know the soil sensitivity which relates the undisturbed shear strength to the disturbed shear strength.

In many offshore locations, the soil undrained shear strength increases with depth. In some locations, a uniform undrained shear strength may be found showing no increase with depth. It is important to model the soil shear strength profile accurately for the purposes of estimating the performance of drag embedment anchors. An undrained shear strength profile which is specific to the location of concern should be used. Where one soil layer overlays another soil layer, it is also important to be able to model the step increase or decrease in undrained shear strength between the different layers. An example of a layered soil shear strength profile is shown in Figure 3.

DEFINITION OF ANCHOR GEOMETRY

The most difficult part of the calculation procedure put forward in this paper is the determination of simplified anchor geometry characteristics. Most modern anchors have rather complicated geometries. It is necessary to simplify these geometries in order to apply the calculation procedure for determination of geotechnical and other forces acting upon the anchor. Figure 4 shows the principal characteristics of a drag embedment anchor in terms of this simplified geometry. The main embedment forces that come onto the anchor are represented by normal, or inverted, bearing pressure forces on the anchor flukes. Consequently, the anchor fluke area, Af, must be defined. The center of this area, at location f1 on Figure 4 must be found. Next the distance from this center, f1, to the anchor shackle point, A, in Figure 4, must be found. For convenience, a nominal zero line is defined going through the shackle point, A. The angle that the line joining the anchor center of area to the shackle point makes with this nominal zero line is then defined as af1.

The principal resistance to anchor dragging comes from the shear forces over the fluke area, Af, and over the shank shear area, As1, shown in Figure 4. Hence, it is necessary to determine the area, As1, and the location of its center at s1. The distance from S1 to A is then defined and the angle relative to the nominal zero line, as1, is found. In addition to the shear forces on the fluke and the shank, there are normal forces or bearing forces on both the shank projected area, As2, and the fluke projected area, Af2. The location of the center of area As2 must be defined. This center is labeled s2 in Figure 4 and the angle that the line form s2 through A makes with the nominal zero line is labeled as2 in this same figure.

Once the above values have all been determined, the solution technique is to apply geotechnical forces at each of the centers of area and to perform a moment balance about the anchor shackle point, A, as shown schematically in Figure 5. The equation to determine the moment, M, about the anchor shackle point is set out below:

$$M = F1.L1 - (F2s + F2n).L2 - F3.L3 - F4.L4 \quad (5)$$

Where F1 through F4 are forces shown on Figure 5, and L1 through L4 are the respective lever arms which can be found from the previously defined angles and distances.

Normally, this equation will result in an unbalanced moment about A while the anchor is beginning to embed. This unbalanced moment will cause the anchor to rotate about the shackle point as it simultaneously drags horizontally and digs in further vertically. The procedure is to assume that the direction of anchor travel between each successive calculation step is parallel to the angle of the fluke. The anchor is considered to be moving through a plastic medium. In a similar manner to the estimation of jack-up spud can resistance to penetration, the disturbed undrained shear strength of the soil is used to calculate the forces defined in Figure 3, at each calculation step.

It is important to note that for the anchor shank shear area, all surfaces of the anchor shank where shear forces may apply, must be considered when the anchor shank area is defined. For twin shank anchors where the shanks are parallel, this means that there is shear force applied on the inside and outside faces of the shanks. Where the shanks are not parallel, a judgment must be made as to whether

it is more appropriate to increase the shank projected area and to decrease the shank shear area. It is inevitable that at least two faces on any twin shank anchor will be exposed to soil shear forces.

It is generally considered that the shear forces acting on the anchor fluke act principally over the top surface of the fluke. Depending upon the fluke geometry, there may be little or no shear forces by the cohesive soil to the back, or bottom, of the anchor fluke.

GENERAL METHOD OF SOLUTION

Horizontal, vertical, and rotational anchor movement is calculated is steps from the initial starting position. The length of the displacement step is equal to a value which must be defined by the user of the method. The direction of the movement is generally parallel to the fluke angle of the anchor calculated at the previous step. The rotation at each step is in a direction which is dependent upon the sign of the moment of geotechnical forces about the anchor shackle (see Figure 5). The magnitude of the rotation at each step must be set by the user of the method in the same way as the displacement step must be set. Horizontal movement continues from step to step while the applied horizontal load at the anchor shackle is greater than the anchor horizontal resistance. This horizontal motive load is calculated from the previously calculated mooring line profile for the specific depth of the shackle at each step.

As the anchor flukes approach a horizontal angle the normal force on the flukes resisting uplift and horizontal movement is reduced. Rotation of the flukes past horizontal causes the normal force on the top of the flukes to reduce to a very low value if horizontal movement is still occuring, and applied horizontal loads are well in excess of vertical loads. This will normally result in reversal of the rotating moment about the anchor shackle, and the flukes will rotate back again. In this manner an equilibrium angle for the anchor is found.

Experience with applying the method suggests that a drag increment of around one-third of the anchor fluke length will result in a satisfactory and stable solution. An angle change increment of around one-half degree also appears to result in satisfactory and stable solutions, when accompanied with the above drag increment.

CALIBRATION OF THE METHOD

The method as set out in this paper has been embodied into a computer program which has been calibrated against large scale anchor tests in the Gulf of Mexico. It is noted that there are two terms which must be set by the user of this approach which are the drag increment between successive calculation steps and the maximum angle change permitted for the anchor between successive calculation steps. Using the empirical guidelines of drag increment equal to one-third of the anchor fluke length and accompanying angle change increment of one-half degree, it is considered that there are only two further parameters that should need to be adjusted in order to calibrate the approach. The first such parameter should match the measured drag distance against the predicted drag distance and is therefore a calibration factor on the drag increment selected by the user. The second calibration factor is for the disturbed value of soil undrained shear strength as used by the program. This is not so much a calibration factor as an adjustment to the soil properties which were assumed in the original large scale tests.

RESULTS

Figures 6, 7, and 8 show some typical results from applying the program to a particular anchor type in a particular soil profile. The soil shear strength profile is as shown in Figure 3. Figure 6 shows the vertical and horizontal forces acting at the anchor. The upper line shows the horizontal force which is available at the anchor shackle resulting from the mooring line tension applied above the sea bed. As the anchor embeds deeper, the horizontal component of force at the anchor shackle is reduced as a consequence of geotechnical forces acting on the line which is further buried with continuing anchor embedment. The line beneath the upper line shows the horizontal force available to resist mooring line applied horizontal forces. This line increases as the anchor embeds deeper. A relatively large increase occurs suddenly at the point where the anchor flukes begin penetration into the stronger layer beneath the surface soil layer. The lowest line on Figure 6 shows the vertical component of force available at the anchor shackle which comes from the mooring line. It is seen that the vertical component of force increases as the anchor drags deeper. The line on Figure 6 above the lowest line represents the anchor capacity available to resist vertical, or uplift forces. A relatively large and sudden increase in this term occurs as the anchor flukes begin penetrating the stronger soil layer.

It can be seen on Figure 6 that the upper line and the line beneath it meet. This represents the point at which maximum horizontal capacity of the anchor has been achieved. The applied horizontal load at the anchor is approximately equal to the maximum resistance that the anchor can provide to horizontal forces. In Figure 7, it is seen that the anchor trajectory becomes horizontal at the point where the applied horizontal load is approximately equal to the horizontal resistance of the anchor.

The upper line of Figure 7 is the anchor trajectory. This line is plotted for the trajectory of the anchor shackle point. The line beneath this upper line on Figure 7 shows the angle of the anchor. This angle steadily increases until the fluke is approximately horizontal. The line for the angle of the anchor then remains at a constant value (with some minor numerical oscillations). The bottom line on Figure 7 shows the angle of the line at the anchor shackle.

After the flukes have reached their equilibrium position (at a drag distance of approximately 230 feet), the anchor still continues to embed and the angle of the mooring line at the anchor shackle continues to increase. At around a drag distance of 350 feet, the anchor has reached its maximum burial depth and further dragging continues in a horizontal direction only. The angle of the mooring line at the anchor shackle after the 350 foot drag distance has been achieved remains constant (with some minor numerical oscillations about a fixed value).

Figure 8 shows a side view of the mooring line geometry when the anchor has reached its final maximum drag depth. The lower line on Figure 8 represents the geometry of the mooring line, while the upper line on Figure 8 represents the mooring line angle. Both curves are plotted against distance from the anchor shackle.

The calibrated Vryhof 7-ton anchor (as tested by Omega Marine in the Gulf of Mexico in 1990) has been studied for capacities vs. mooring line touchdown angle at the sea bed. This touchdown angle has been varied from zero degrees (as tested) to 20 degrees in five degree steps, and the maximum holding capacity of the system is shown tabulated in Table 1. To produce the results in Table 1, a constant line load of 200 kips has been used. The horizontal load component is a function of the cosine of the touchdown angle. The results show that the maximum horizontal load that can be resisted by the anchor is strongly dependent upon this touchdown angle for a given line tension.

Sensitivity of anchor capacity to the soil shear strength gradient is shown in Table 2. The calibrated Vryhof 2-ton anchor results have been used to produce Table 2. The soil shear strength gradient has been varied from a 7.5 lb. line to a 15 lb. line. This means that the soil shear strength increases linearly with depth at a rate of, for example, 7.5 lbs/square foot per foot of depth. In order to produce Table 2, a horizontal line load at the sea bed has been assumed. The results in Table 2 are expressed as a percentage of the maximum values found for a 10 lb. soil.

Table 3 has been produced in order to show the variation of anchor capacity when chain is used as opposed to wire (wire forerunners were used for the 1990 large scale tests). The results in Table 3 show the various percentages of the horizontal system capacity and vertical system capacity coming from the anchor part of the system alone, and the wire or chain part of the system alone. Results are normalized to the capacity of the system using 3.5 inch diameter wire rope.

CONCLUSIONS

A method for simplifying the important components of anchor geometry has been presented. A method for assessing the geotechnical forces acting on this geometry as anchor embedment occurs during anchor dragging has been presented. A method for assessing the kinematic performance of the anchor during embedment has been described which accounts for geotechnical forces on the anchor, geotechnical forces on the mooring line as it is embedded by the anchor, and the weight of both the mooring line and the anchor. It is concluded that the approach produces reasonable results when compared to large scale tests. It is further concluded that the method permits the prediction of anchor capacities in different soil conditions (for cohesive soils only at the present time).

It is concluded that the method, when embodied into a computer program, will permit the optimization of anchor designs for particular soil conditions. This will result in cost savings for anchors designed for both permanent mooring systems in deep water and for anchors designed for temporary mooring systems for mobile rigs and other offshore floating vessels. It is further concluded that the method permits a rational comparison of the anchor capacities to be expected where wire rope is used instead of chain or vice versa.

REFERENCES

1. Puech, A., "The Use Of Anchors In Offshore Petroleum Operations", Gulf Publishing Company, 1984.

2. Vivatrat, V., Valent, P.J., and Ponterio, A.A., "The Influence Of Chain Friction On Anchor Pile Design", OTC 4178, Offshore Technology Conference, May 1982.

3. Stewart, W.P., True, D., and Jones, T., "Deep Embedment Plate Anchors", OTC 6033, Offshore Technology Conference, May 1989.

4. Dutta, A., and Degenkamp, G., "Behavior Of Embedded Mooring Chains In Clay During Chain Tensioning", OTC 6031, Offshore Technology Conference, May 1989.

TABLE 1: ANCHOR SYSTEM CAPACITY VS. LINE ANGLE

angle	%age max. line load	%age max. horiz. load
0	100	100
5	98	98
10	90	89
15	75	72
20	55	52

Note that basic case is for horizontal load. Inclined loads are factored by the cosine of the inclination angle to obtain the horizontal load component. For example, a 200 kip horizontal applied load at 20 degrees is equivalent to a line load of 213 kips.

TABLE 2: ANCHOR SYSTEM CAPACITY VS SOIL STRENGTH

soil gradient	%age max. load	%age shackle depth
7.5–lb	68	89
10–lb	100	100
12.5–lb	121	100
15–lb	141	100

TABLE 3: ANCHOR SYSTEM CAPACITY VS. LINE SIZE AND TYPE

SIZE	%age Htot	%age A	%age L	%age depth	%age drag
3.5″ wire	100	100	100	100	100
3.0″ chain	59	54	72	50	52
3.5″ chain	55	50	68	45	41
4.0″ chain	53	46	72	41	34

In the above table the following definitions are used:
%age Htot = percentage of horizontal system capacity with wire
%age A = percentage of anchor part of system capacity with wire
%age L = percentage of line part of system capacity with wire
%age depth = percentage of maximum shackle embedment depth with wire
%age drag = percentage of wire drag distance to achieve max. capacity

Forces On Buried Section of Anchor Line

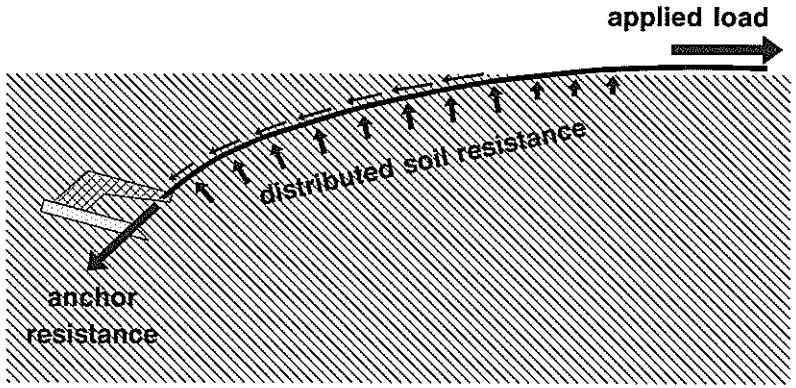

FIGURE 1

Forces on Buried Anchor Line Element

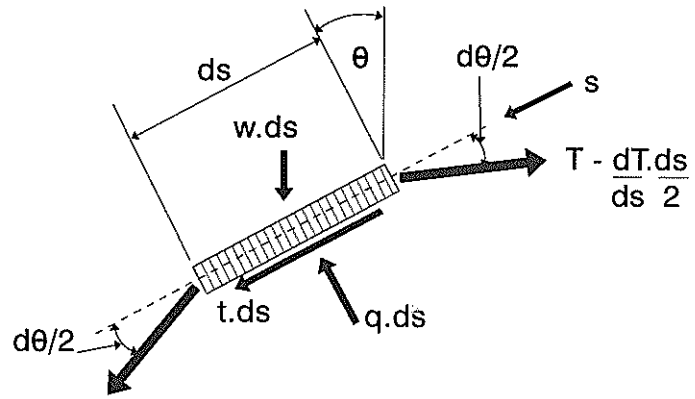

FIGURE 2

SOIL STRENGTH PROFILES

Provided that the values of Cu are all positive they may be any values, and do not need to increase with depth, as shown here.

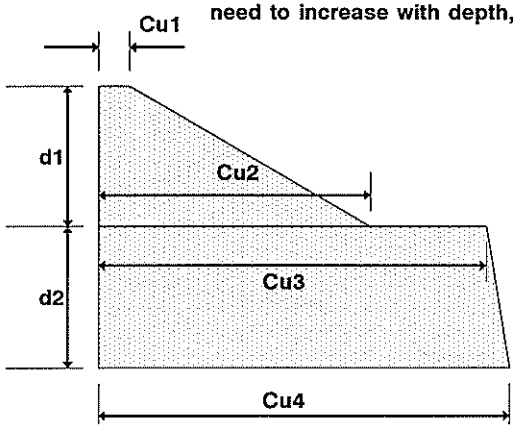

FIGURE 3

Anchor Nomenclature & Geometry

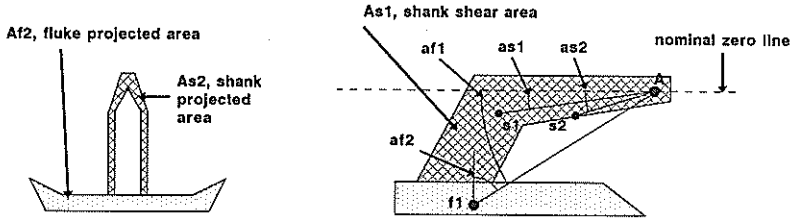

KEY
f1 = fluke center of area
s1 = shank center of shear area
s2 = shank center of normal area
lf = fluke distance from A to f1
ls1 = 1st shank distance from A to s1
ls2 = 2nd shank distance from A to s2
af1 = 1st fluke angle
af2 = 2nd fluke angle
as1 = 1st shank angle
as2 = 2nd shank angle
nominal zero line does not have to be parallel to fluke, as shown above.

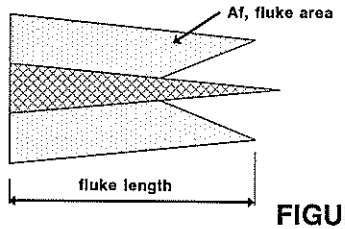

FIGURE 4

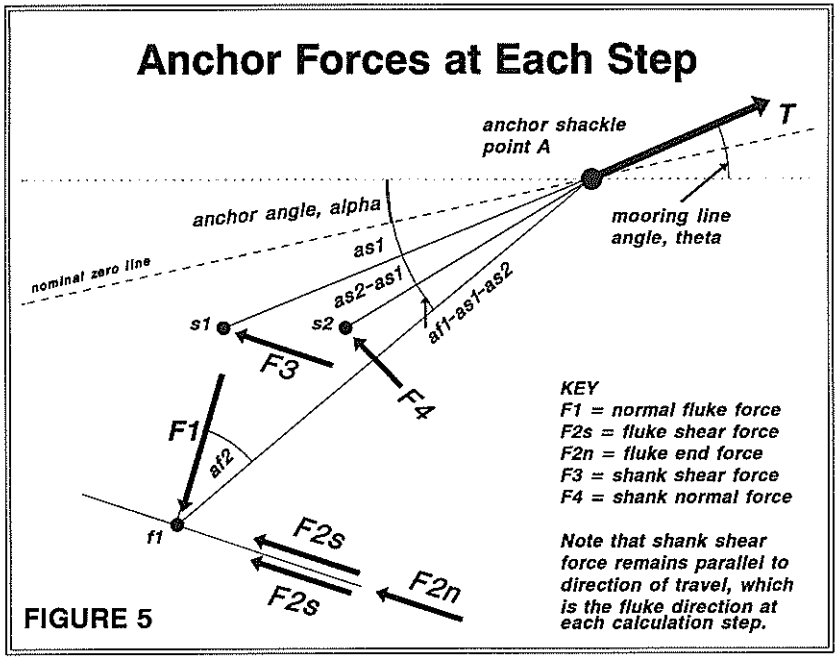
Anchor Forces at Each Step
anchor shackle point A
T
anchor angle, alpha
mooring line angle, theta
nominal zero line
as1
as2-as1
af1-as1-as2
s1
s2
F3
F4
F1
af2
f1
F2s
F2s
F2n
KEY
F1 = normal fluke force
F2s = fluke shear force
F2n = fluke end force
F3 = shank shear force
F4 = shank normal force
Note that shank shear force remains parallel to direction of travel, which is the fluke direction at each calculation step.
FIGURE 5

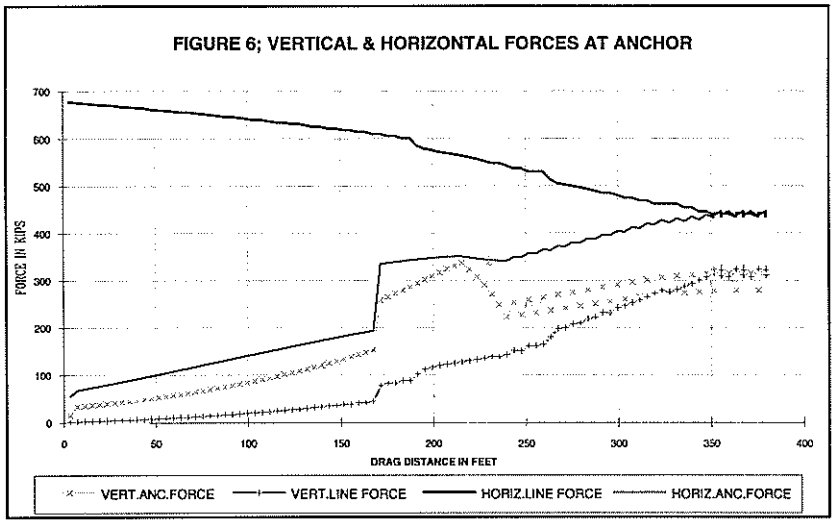
FIGURE 6; VERTICAL & HORIZONTAL FORCES AT ANCHOR
FORCE IN KIPS
DRAG DISTANCE IN FEET
VERT.ANC.FORCE
VERT.LINE FORCE
HORIZ.LINE FORCE
HORIZ.ANC.FORCE

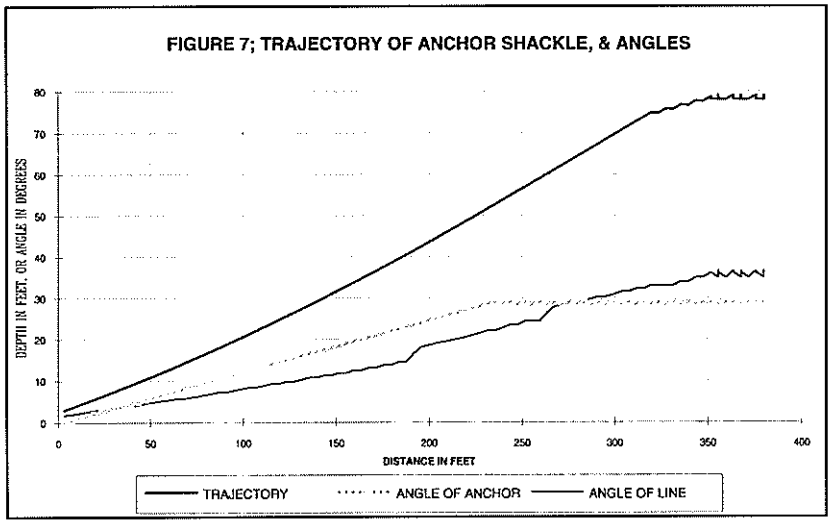
FIGURE 7; TRAJECTORY OF ANCHOR SHACKLE, & ANGLES
DEPTH IN FEET, OR ANGLE IN DEGREES
DISTANCE IN FEET
TRAJECTORY
ANGLE OF ANCHOR
ANGLE OF LINE

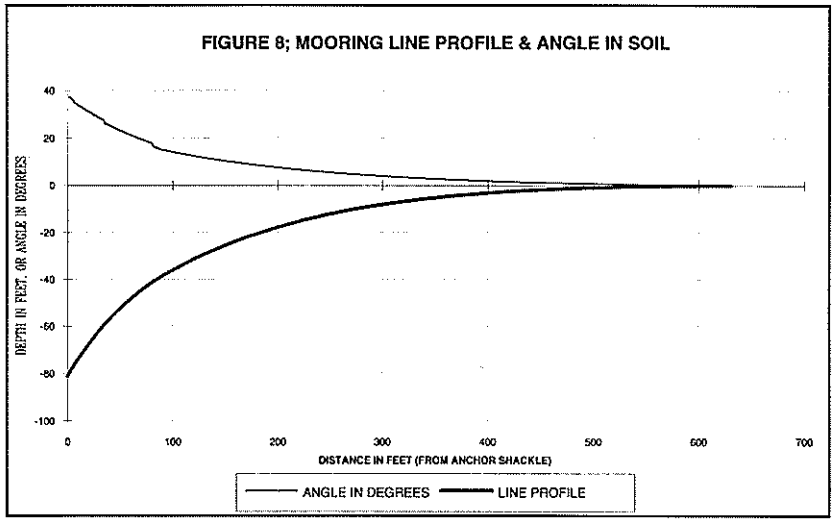
FIGURE 8; MOORING LINE PROFILE & ANGLE IN SOIL
DEPTH IN FEET, OR ANGLE IN DEGREES
DISTANCE IN FEET (FROM ANCHOR SHACKLE)
ANGLE IN DEGREES
LINE PROFILE